Mathematical Biosciences and Engineering

https://www.aimspress.com/journal/mbe

MBE, 23(x): 1774–1798.
DOI: 10.3934/mbe.2026065
Received: 22 December 2025
Revised: 20 April 2026
Accepted: 07 May 2026
Published: 22 May 2026 2026

Research article

X–factorable transformation–based control of interconnected Lotka–Volterra systems

Lőrinc Márton[1] **and Katalin M. Hangos**[2,3]

[1] Department of Electrical Engineering, Sapientia Hungarian University of Transylvania, Corunca, Romania

[2] Systems and Control Laboratory, HUN-REN Institute for Computer Science and Control, Budapest, Hungary

[3] Department of Electrical Engineering and Information Systems, University of Pannonia, Veszprém, Hungary

* **Correspondence:** Email: martonl@ms.sapientia.ro.

Abstract: A dynamic model of interconnected Lotka–Volterra systems has been developed both with static and delayed interconnections. We have shown that the X-transformed model of interconnected Lotka–Volterra systems naturally admits a quasi-polynomial (QP) representation, facilitating systematic analysis and control design. In order to analyze local asymptotic stability around a positive equilibrium, we have shown that the X-factorable transformation preserves local diagonal stability. We propose a decentralized setpoint-tracking controller design based on the transformed model that guarantees population persistence in the subsystems of the network. The proposed controller design is computationally simple and ensures that the controlled system is locally diagonally stable around the prescribed setpoint. Moreover, larger controller gains improve disturbance attenuation, mitigating the effect of the disturbance offset term on control performance.

Keywords: network dynamics; Lotka-Volterra systems; quasi-polynomial systems; X-factorable transformation; setpoint control

1. Introduction

Positive polynomial systems can model a wide range of physical, chemical, and biological processes, while they form a special class of smooth nonlinear systems. A special subclass of positive polynomial systems, the so-called *Lotka-Volterra systems (LV systems)*, is a popular and well-investigated model class to describe the dynamic behavior of interactive species [1, 2]. These and their generalizations are common model classes of ecological processes.

1.1. Higher order LV models

Although classical Lotka–Volterra (LV) models are capable of describing a broad range of dynamical behaviors, their expressive power is limited when interactions extend beyond pairwise species coupling. This limitation has motivated the development of more sophisticated ecological models that explicitly incorporate higher-order interactions. Such dynamics can be captured by so-called *higher-order Lotka–Volterra systems* (see, e.g., [3–7]), which generalize the classical framework by allowing interactions among three or more species.

The family of *quasi-polynomial (QP) systems* is regarded as a further generalization of the Lotka-Volterra form [8]. The QP system class splits into classes of equivalence, where a dynamically similar Lotka-Volterra model can be constructed from the invariants of the equivalence classes [9]. It has also been shown that a number of non-polynomial positive system models can also be embedded into a QP model form [10].

1.2. Networked LV systems

To describe and analyze spatially distributed ecological systems, the notion of *multi-patch LV systems* has been introduced, where a single population is considered as being made up of a collection of smaller sub-populations living in spatially homogeneous domains, called patches, and the individuals may migrate between the patches; see e.g. [11–13].

Multi-patch ecological systems often exhibit spatially distributed transfer mechanisms, such as population and/or food migration between patches in a convective or diffusive way. Their dynamic behavior can be described using *delayed models with either constant or distributed delays* [14–16]. A two-patch predator-prey system with diffusion and distributed delay was studied in [17]. The modeling of compartmental systems, which are another class of smooth positive nonlinear systems, with distributed delays was discussed, e.g., in [18].

1.3. Stability and controller design

The stability of ecological systems is a fundamental concept in ecology, which offers valuable insights into species coexistence, biodiversity, and community persistence; see [19] for a recent review. Because of the nonlinear and sometimes delayed nature of the system models, advanced special approaches are needed for both their dynamic analyses and controller design.

The stability of QP models can be analyzed using Lyapunov-based methods [20]. Stability analysis of QP models is reported in [21] with applications to biological network models. The embedding of QP models into LV system models is a basis of several recent advanced dynamic analysis and control results in the field, see e.g. [22–24]. Passivity analysis of LV and QP systems has been presented in [25], and it was applied to controller design.

The dynamics and stability of multi-patch LV systems have been investigated by a number of authors (e.g. [12, 26]), and it has been found that the stability depends on both the stability of the patches and that of the network properties.

A substantial body of work has addressed the *control of large-scale interconnected nonlinear systems* through distributed and decentralized frameworks. Early contributions, such as [27], proposed sequential and iterative architectures for distributed model predictive control (MPC), enabling coordinated decision-making while preserving subsystem autonomy. This line of research was further syn-

thesized in the tutorial review by Panagiotis D. Christofides and co-authors in [28], which highlights the theoretical foundations and practical challenges of distributed MPC, including stability, communication constraints, and scalability. More recently, learning-based approaches have been incorporated into decentralized predictive control, as demonstrated in [29], where machine learning techniques are leveraged to approximate nonlinear dynamics and improve control performance.

Several studies have examined *control strategies for interconnected or multi-patch Lotka–Volterra systems*, focusing on how external interventions can enforce coexistence and stability in population dynamics. For instance, impulsive control methods have been developed for high-dimensional Lotka–Volterra models, where species densities are adjusted via discrete impulses applied simultaneously to multiple populations to stabilize a desired positive state and prevent extinction [30]. In another line of work, metapopulation modeling approaches have been proposed to control Lotka–Volterra dynamics across spatially discrete habitat patches: By introducing structured inter-patch migration, the trajectories of each patch's species can be driven to a prescribed coexistence equilibrium [31]. Additionally, feedback control has been incorporated into ratio-dependent predator–prey Lotka–Volterra systems with delay to ensure permanence and global attractivity of positive solutions [32]. The global stability of delayed nonlinear LV systems with feedback control and patch structure is analyzed, e.g., in [33]. A recent paper [34] considers three identical chaotic generalized LV biological systems and proposes a biological adaptive control law for achieving global asymptotic stability of state variables of this system with unknown parameters. These contributions collectively demonstrate the importance of control mechanisms in shaping the long-term behavior of multi-patch and interconnected positive systems.

A decentralized control method is proposed in our recent paper [35], which assures that the states of each Lotka-Volterra system in the networked LV system can be driven into a prescribed setpoint regardless of migration. The results have been generalized to quasi-polynomial systems and networks of Lotka-Volterra systems having interconnections with distributed delay.

1.4. Aim and contributions

Motivated by the results discussed above, the aim of this work is to propose a theoretically grounded yet practically feasible approach for designing controllers that achieve desired dynamical properties in interconnected (networked) Lotka–Volterra systems. In particular, we focus on ensuring persistence, i.e., the avoidance of extinction, across the patches of Lotka–Volterra networks. Our approach leverages the X-factorable transformation framework [36] for both analysis and control design. We also discuss the stability-preserving properties of this model mapping in detail.

The main contributions of this study are summarized as follows:

- We show that the X-factorable transformation preserves local diagonal stability.
- We demonstrate that the X-transformed model of interconnected Lotka–Volterra systems naturally admits a quasi-polynomial (QP) representation, facilitating systematic analysis and control design.
- We propose a decentralized setpoint-tracking controller design based on the transformed model that guarantees population persistence in the subsystems of the network.

1.5. Notations

Let $\mathbb{R}$ denote the set of real numbers, and $\mathbb{R}_{\geq 0} = [0, \infty)$ and $\mathbb{R}_{>0} = (0, \infty)$.
$\mathbf{x} = (x_i) \in \mathbb{R}^n$ is a column vector with n entries such that $x_i \in \mathbb{R},\ \forall i$.
$\mathbf{x} = (x_i) \in \mathbb{R}^n_{\geq 0} \subset \mathbb{R}^n$ such that $x_i \in \mathbb{R}_{\geq 0},\ \forall i$.
$\mathbf{x} = (x_i) \in \mathbb{R}^n_{>0} \subset \mathbb{R}^n$ such that $x_i \in \mathbb{R}_{>0},\ \forall i$.
$\mathbf{0} \in \mathbb{R}^n$ is the zero vector.
$A = (a_{ij}) \in \mathbb{R}^{m\times n}$ is a real-valued matrix with $m \times n$ entries.
A^T is the transpose of A.
$D = \text{diag}(\mathbf{x}) \in \mathbb{R}^{n\times n}$ is a diagonal matrix such that $d_{ii} = x_i$, $\mathbf{x} \in \mathbb{R}^n$.
$I \in \mathbb{R}^{n\times n}$ is the identity matrix.
$O \in \mathbb{R}^{n\times n}$ is the zero matrix.
$\mathbf{x}_1 \circ \mathbf{x}_2 = (x_{1i}x_{2i})$ is the Hadamard (entry-wise) vector product of two vectors with the same dimensions.
$\mathbf{x} < \mathbf{0}$ – entry-wise negative vector.
$A < O$ is a negative definite matrix.
$\text{Ln}(\mathbf{x}) = (\ln(x_i))$ – entry-wise logarithm of a vector.

2. Quasi-polynomial systems and Lotka-Volterra networks

2.1. Quasi-polynomial systems

Consider the following dynamical system:

$$\dot{\mathbf{x}} = \mathbf{x} \circ (\mathcal{A}\mathbf{q} + \mathbf{s}), \quad \mathbf{x}(0) = \mathbf{x}_0 \in \mathbb{R}^m_{\geq 0}, \tag{2.1}$$

where $\mathbf{x} \in \mathbb{R}^m$ is the state vector, $\mathbf{x}_0$ is the constant vector of the initial state, $\mathcal{A} \in \mathbb{R}^{p\times m}$ is the matrix of interaction coefficients, and $\mathbf{s} \in \mathbb{R}^m$ is the vector of rate coefficients. $\mathbf{q}(\cdot) : \mathbb{R}^m \to \mathbb{R}^p$ is a vector function, the so-called monomial function, in which each entry has the form:

$$q_j = \prod_{k=1}^{m} x_k^{\mathcal{B}_{jk}} \quad , \quad j = 1, ..., p, \tag{2.2}$$

where the exponent matrix is $\mathcal{B} \in \mathbb{R}^{p\times m}$. Note that $p \geq m$ in these models.

These systems are *nonnegative*, in the sense that $\mathbf{x}_0 \in \mathbb{R}^m_{\geq 0}$ implies that $\mathbf{x}(t) \in \mathbb{R}^m_{\geq 0}, \forall t > 0$.

Such systems are called quasi-polynomial (QP) systems [9].

2.2. Lotka-Volterra systems

The Lotka-Volterra (LV) models are a special type of quasi-polynomial systems, originally introduced to model the population dynamics of coexisting biological species [1]. They are described by the following ODE (ordinary differential equation):

$$\dot{\mathbf{x}} = \mathbf{x} \circ (M\mathbf{x} + \mathbf{r}), \quad \mathbf{x}(0) = \mathbf{x}_0 \in \mathbb{R}^m_{\geq 0}. \tag{2.3}$$

The matrix $M \in \mathbb{R}^{m\times m}$ contains the interaction coefficients and $\mathbf{r} \in \mathbb{R}^m$ is a rate coefficient vector.

The entries of the state vector are typically interpreted as the expected population sizes of the respective species.

It is important to note that LV models in Eq. (2.3) are special forms of QP models in Eqs. (2.1) and (2.2) such that

$$\mathcal{A} = M \ , \ \mathcal{B} = I \ , \ \mathbf{q} = \mathbf{x} \ , \ \mathbf{s} = \mathbf{r} \ , \ m = p. \tag{2.4}$$

The trivial *equilibrium point* of the system (2.3) is $\mathbf{x}^* = \mathbf{0}$. The non-trivial equilibrium points, when they exist, are the solution of the following linear system:

$$M\mathbf{x}^* = -\mathbf{r}. \tag{2.5}$$

The *(global) asymptotic stability* of a nontrivial equilibrium state $\mathbf{x}^*$ can be analyzed by considering the Lyapunov function candidate:

$$L = \sum_{i=1}^{m} \lambda_i \left(x_i - x_i^* - x_i^* \ln\left(\frac{x_i}{x_i^*}\right)\right), \quad \lambda_i > 0. \tag{2.6}$$

See, e.g., [21].

A matrix M is called *diagonally stable* if

$$\Lambda M + M^T \Lambda < O. \tag{2.7}$$

where $\Lambda = \text{diag}\,(\lambda_i) > O$.

By direct computation, it follows that system (2.3) is asymptotically stable, i.e. $\dot{L} < 0 \ \forall \mathbf{x} \neq \mathbf{0}$ if M is diagonally stable.

Persistency: The Lotka-Volterra system is called persistent if $x_{i0}(t) \geq 0$, which implies $x_i(t) \geq \varepsilon > 0, \ \forall t > 0, \ i = 1, \ldots, m$.

If all the non-trivial equilibrium states are asymptotically stable, the system is also persistent. Otherwise, if $\exists \ x_i^* \leq 0$, the asymptotic stability does not imply persistency.

Higher order Lotka Volterra systems are a class of QP systems in which the exponents ($\mathcal{B}_{jk}$) are non-negative integer values. In such Lotka-Volterra type systems, higher-order polynomial or quasi-polynomial interactions are also considered. The second-order Lotka-Volterra model reads as:

$$\dot{x}_i = x_i \left(r_i + \sum_j a_j x_j + \sum_{j,k} b_{jk} x_j x_k \right), \quad i, j, k = 1 \ldots m. \tag{2.8}$$

Such systems have important applications in theoretical ecology, where higher-order interactions play a critical role in shaping community structure and stability [3, 4]. They are used to model complex ecological processes such as multi-species competition, facilitation, and nonlinear trophic effects that cannot be captured by classical Lotka–Volterra formulations.

2.3. QP embedding into LV systems

It is known that each positive quasi-polynomial system can be embedded into a Lotka-Volterra system (2.3) of sufficiently high order [37].

The embedding can be performed by first forming the so-called *logarithmic form of QP models*. The model in Eqs (2.1)-(2.2) can also be written as

$$\begin{array}{l} \frac{d\text{Ln}(\mathbf{x})}{dt} = \mathcal{A}\mathbf{q} + \mathbf{s}, \\ \text{Ln}(\mathbf{q}) = \mathcal{B}\text{Ln}(\mathbf{x}). \end{array} \tag{2.9}$$

Multiplying the first equation above by the constant matrix $\mathcal{B}$ and substituting the second algebraic equation into it, we arrive at the following LV model:

$$\frac{d\mathrm{Ln}(\mathbf{q})}{dt} = \mathcal{B}\mathcal{A}\mathbf{q} + \mathcal{B}\mathbf{s} = \mathcal{M}\mathbf{q} + \mathbf{r}, \tag{2.10}$$

where $\mathcal{M} = \mathcal{B}\mathcal{A}$ and $\mathbf{r} = \mathcal{B}\mathbf{s}$.

It is important to note that in the case of $p > m$ (i.e. more quasi-monomials than state variables), the parameter matrix $\mathcal{M}$ of the above LV form is rank deficient even in the case when $\mathrm{rank}(\mathcal{B}) = m$ (i.e. $\mathcal{B}$ is of full rank).

More discussion on the properties of an LV model that resulted from the embedding can be found in [38].

2.4. Interconnected Lotka-Volterra systems

Let us consider a number of n patches in which the interactions of the species population are described by Lotka-Volterra models as follows:

$$\dot{\mathbf{x}}^{(j)} = \mathbf{x}^{(j)} \circ \left(M^{(j)}\mathbf{x}^{(j)} + \mathbf{r}^{(j)}\right), \;\; \mathbf{x}^{(j)}(0) = \mathbf{x}_0^{(j)} \in \mathbf{R}^m_{\geq 0}. \tag{2.11}$$

Here, $\mathbf{x}^{(j)} \in \mathbb{R}^m_{\geq 0}$ is the state vector in which each entry represents a species population size in the jth patch.

The interconnections among the Lotka-Volterra subsystems are modeled similarly as in [35], allowing a slightly more general interconnection structure. The interconnections among the patches are considered to be described by a directed graph $\mathcal{G}$ in which the nodes represent the patches, while the edges represent the directed interconnections between them. If there is a directed edge from node i to node j, a directed population flow is allowed from node i to node j. Bidirectional population flows are also allowed between patches. Such cases are represented by a pair of directed edges with opposite directionality between the two corresponding patches.

Let us introduce the following notations:

- $\mathcal{N}_I^{(j)}$ - input neighbor set of the node j: $i \in \mathcal{N}_I^{(j)}$ if there is a directed flow from the ith patch to the jth patch.
- $\mathcal{N}_O^{(j)}$ - output neighbor set of the node j: $i \in \mathcal{N}_O^{(j)}$ if there is a directed flow from the jth patch to the ith patch.

The population dynamics in the jth patch is modeled as:

$$\dot{\mathbf{x}}^{(j)} = \mathbf{x}^{(j)} \circ \left(M^{(j)}\mathbf{x}^{(j)} + \mathbf{r}^{(j)}\right) + \mathbf{v}_I^{(j)} - \mathbf{v}_O^{(j)}, \;\; \mathbf{x}^{(j)}(0) = \mathbf{x}_0^{(j)}, \tag{2.12}$$

where $\mathbf{v}_I^{(j)} \in \mathbb{R}^m_{\geq 0}$ is the input flow rate and $\mathbf{v}_O^{(j)} \in \mathbb{R}^m_{\geq 0}$ is the output flow rate of the jth patch.

It is considered that the population *outflow rate* from each patch is proportional to the population size in each patch, i.e. $\mathbf{v}_O^{(j)} = \mathbf{b}^{(j)} \circ \mathbf{x}^{(j)}$, where $\mathbf{b}^{(j)} = (\beta_\ell^{(j)}) \in \mathbb{R}^m_{\geq 0}$ is the vector of output migration coefficients.

The population outflow reaches the patches from the set $\mathcal{N}_O^{(j)}$. Assign a weighted adjacency matrix $\alpha = (\alpha_{ij}) \in \mathbb{R}^{n\times n}_{\geq 0}$ to the interconnection graph $\mathcal{G}$ in the form

$$\alpha_{ij} = \begin{cases} \alpha_{ij} \in (0, 1], & \text{if } i \in \mathcal{N}_I^{(j)} \text{ or } j \in \mathcal{N}_O^{(i)}, \\ 0, & \text{otherwise.} \end{cases} \tag{2.13}$$

The parameters α_{ij} are called *fraction coefficients*, and they satisfy the relation

$$\sum_{j\in\mathcal{N}_O^{(i)}} \alpha_{ij} = 1. \tag{2.14}$$

Using the fraction coefficients, the outflow rate has the following form:

$$\mathbf{v}_O^{(j)} = \sum_{i\in\mathcal{N}_O^{(j)}} \alpha_{ij}\mathbf{b}^{(j)} \circ \mathbf{x}^{(j)} = \mathbf{b}^{(j)} \circ \mathbf{x}^{(j)}. \tag{2.15}$$

The *inflow rates* read as

$$\mathbf{v}_I^{(j)} = \sum_{i\in\mathcal{N}_I^{(j)}} \alpha_{ij}\mathbf{v}_O^{(i)} = \sum_{i\in\mathcal{N}_I^{(j)}} \alpha_{ij}\mathbf{b}^{(j)} \circ \mathbf{x}^{(i)}. \tag{2.16}$$

By applying the proposed interconnection approach, the population dynamics in the jth patch model reads as:

$$\dot{\mathbf{x}}^{(j)} = \mathbf{x}^{(j)} \circ \left(M^{(j)}\mathbf{x}^{(j)} + \mathbf{r}^{(j)}\right) - \mathbf{b}^{(j)} \circ \mathbf{x}^{(j)} + \sum_{i\in\mathcal{N}_I^{(j)}} \alpha_{ij}\mathbf{b}^{(i)} \circ \mathbf{x}^{(i)}, \tag{2.17}$$

$$\text{i.e. } \dot{x}_\ell^{(j)} = \sum_{k=1}^{m} M_{\ell k}^{(j)} x_\ell^{(j)} x_k^{(j)} + r_\ell^{(j)} x_\ell^{(j)} - \beta_\ell^{(j)} x_\ell^{(j)} + \sum_{i\in\mathcal{N}_I^{(j)}} \alpha_{ij}\beta_\ell^{(i)} x_\ell^{(i)}.$$

It is important to note that the population dynamics model (2.17) in the jth path is not a Lotka-Volterra model anymore due to the last inflow term.

The global model. Taken for every patch, the dynamic behavior of the interconnected Lotka-Volterra system can be formulated as

$$\dot{\mathbf{x}} = \mathbf{x} \circ (\mathbf{M}\mathbf{x} + \mathbf{r}) + \mathbf{L}\mathbf{x}, \tag{2.18}$$

where

$$\begin{aligned} \mathbf{x} &= (\mathbf{x}^{(1)T} \ \dots \ \mathbf{x}^{(n)T})^T \\ \mathbf{r} &= (\mathbf{r}^{(1)T} \ \dots \ \mathbf{r}^{(n)T})^T \\ \mathbf{M} &= \operatorname{diag}\left(M^{(1)} \ \dots \ M^{(n)}\right) \\ \mathbf{L} &= \mathbf{L}_I - \mathbf{L}_O. \end{aligned} \tag{2.19}$$

Here,

$$\mathbf{L}_I = \begin{pmatrix} O & \alpha_{21}\operatorname{diag}\left(\mathbf{b}^{(2)}\right) & \dots & \alpha_{n1}\operatorname{diag}\left(\mathbf{b}^{(n)}\right) \\ \alpha_{12}\operatorname{diag}\left(\mathbf{b}^{(1)}\right) & O & \dots & \alpha_{n2}\operatorname{diag}\left(\mathbf{b}^{(n)}\right) \\ \dots & \dots & \dots & \dots \\ \alpha_{1n}\operatorname{diag}\left(\mathbf{b}^{(1)}\right) & \alpha_{2n}\operatorname{diag}\left(\mathbf{b}^{(2)}\right) & \dots & O \end{pmatrix}, \tag{2.20}$$

$$\mathbf{L}_O = \operatorname{diag}\left(\mathbf{b}^{(1)T} \ \dots \ \mathbf{b}^{(n)T}\right).$$

In the *interconnection matrix* $\mathbf{L}$, the column sums are 0; see Eq. (2.14). This implies that the outflow from the jth patch must reach the patches in $\mathcal{N}_O^{(j)}$.

Positive equilibrium states ($\mathbf{x}^{(j)*} \in \mathbb{R}^m_{>0}$). By (2.17), the equilibrium states of the subsystems should satisfy:

$$\left(M^{(j)}\mathbf{x}^{(j)*} + \mathbf{r}^{(j)} - \mathbf{b}^{(j)}\right) \circ \mathbf{x}^{(j)*} + \sum_{i \in \mathcal{N}_I^{(j)}} \alpha_{ij}\mathbf{b}^{(i)} \circ \mathbf{x}^{(i)*} = \mathbf{0},\ i = 1 \dots n. \tag{2.21}$$

The system (2.21) is quadratic. Methods for the calculation of non-zero roots of higher order Lotka-Volterra systems (i.e. quadratic QP systems) are discussed, e.g., in [3].

From Eq (2.17), it can be seen that when all Lotka-Volterra subsystems are identical and the network is balanced, i.e. $\mathbf{b}^{(j)} = \sum_{i \in \mathcal{N}_I^{(j)}} \alpha_{ij}\mathbf{b}^{(i)}$, the equilibrium state will be the same as in the connected case.

When a subsystem does not have inflow ($\mathcal{N}_I^{(j)} = \emptyset$), the subsystem model reduces to a harvested Lotka-Volterra model, and for large entries in $\mathbf{b}^{(j)}$, non-positive steady-state values may emerge.

Generally, it can be affirmed that, when the population outflow is greater than the population inflow in a subsystem, non-positive or near-zero equilibrium states may appear with higher probability. This is illustrated by the example below.

Example 1. *Consider two 2-dimensional Lotka-Volterra systems that are interconnected by a bidirectional migration channel, as presented in Eq.* (2.17)*. In the model,* $\mathbf{b}^{(1)} = (\beta_1\ \beta_1)^T$*, and* $\mathbf{b}^{(2)} = (\beta_2\ \beta_2)^T$*. The models of these interconnected systems read as:*

$$\begin{pmatrix} \dot{x}_1^{(1)} \\ \dot{x}_2^{(1)} \end{pmatrix} = \begin{pmatrix} x_1^{(1)} \\ x_2^{(1)} \end{pmatrix} \circ \left(\begin{bmatrix} m_{11}^{(1)} & m_{12}^{(1)} \\ m_{21}^{(1)} & m_{22}^{(1)} \end{bmatrix} \begin{pmatrix} x_1^{(1)} \\ x_2^{(1)} \end{pmatrix} + \begin{pmatrix} r_1^{(1)} - \beta_1 \\ r_2^{(1)} - \beta_1 \end{pmatrix} \right) + \alpha_{21}\beta_2 \begin{pmatrix} x_1^{(2)} \\ x_2^{(2)} \end{pmatrix}, \tag{2.22}$$

$$\begin{pmatrix} \dot{x}_1^{(2)} \\ \dot{x}_2^{(2)} \end{pmatrix} = \begin{pmatrix} x_1^{(2)} \\ x_2^{(2)} \end{pmatrix} \circ \left(\begin{bmatrix} m_{11}^{(2)} & m_{12}^{(2)} \\ m_{21}^{(2)} & m_{22}^{(2)} \end{bmatrix} \begin{pmatrix} x_1^{(2)} \\ x_2^{(2)} \end{pmatrix} + \begin{pmatrix} r_1^{(2)} - \beta_2 \\ r_2^{(2)} - \beta_2 \end{pmatrix} \right) + \alpha_{12}\beta_1 \begin{pmatrix} x_1^{(1)} \\ x_2^{(1)} \end{pmatrix}. \tag{2.23}$$

Note that $\alpha_{21} = \alpha_{12} = 1$.

Let's consider the parameters: $m_{11}^{(1)} = m_{22}^{(1)} = m_{11}^{(2)} = m_{22}^{(2)} = 0$, $m_{12}^{(1)} = m_{12}^{(2)} = -1$, $m_{21}^{(1)} = m_{21}^{(2)} = 1$, $r_1^{(1)} = r_1^{(2)} = 0.3$*, and* $r_2^{(1)} = r_2^{(2)} = -0.3$*. With this choice of parameters, each subsystem corresponds to a classic Lotka-Volterra predator-prey model.*

If $\beta_1 = \beta_2 = 0$*, then* $\mathbf{x}^{(1)*} = \mathbf{x}^{(2)*} = (0.3\ \ 0.3)^T$*, and the disconnected subsystems have positive equilibrium.*

Now consider the case $\beta_1 = 0.01$, $\beta_2 = 0.5$*. Then, an equilibrium solution is* $\mathbf{x}^{(1)*} = (0.3036\ \ 0.3145)^T$, $\mathbf{x}^{(2)*} = (0.0149\ \ -0.0040)^T$*. The equilibrium points were computed using a numerical solver – "fsolve" MATLAB function – with* $1E-12$ *absolute precision. For the iterative numerical solver, the initial values were chosen as* $\mathbf{x}^{(1)}[0] = \mathbf{x}^{(2)}[0] = (0.5\ \ 0.5)^T$.

Hence, due to the asymmetric migration flows, population extinction in the second patch is expected.

Now, let's assume that all subsystems (2.21) admit positive solutions. Then, $\exists\, \mathbf{t}_{ij} \in \mathbb{R}^m_{>0}$ with strictly positive entries such that

$$\mathbf{x}^{(i)*} = \mathbf{t}_{ij} \circ \mathbf{x}^{(j)*},\ \ \forall i, j. \tag{2.24}$$

In this case, the equilibrium state of the jth subsystem is the solution of:

$$\left(M^{(j)}\mathbf{x}^{(j)*} + \mathbf{r}^{(j)} - \mathbf{b}^{(j)}\right) \circ \mathbf{x}^{(j)*} + \sum_{i \in \mathcal{N}_I^{(j)}} \alpha_{ij}\mathbf{b}^{(i)} \circ \mathbf{t}_{ij} \circ \mathbf{x}^{(j)*} = \mathbf{0}. \tag{2.25}$$

Generally, the vectors $\mathbf{t}_{ij}$ are unknown. However, this model representation becomes particularly useful when prescribing equilibrium states through control is desired.

The interconnected Lotka–Volterra network model in (2.17) does not exhibit a quasi-polynomial structure due to the presence of population inflow terms. Nevertheless, as shown in the following section, an appropriate transformation can be introduced that restores a QP representation, thereby enabling the systematic application of QP-based analysis and control design techniques to this class of networks.

3. X-factorable transformation and diagonal stability

Let a dynamic system

$$\dot{\mathbf{x}} = \mathbf{f}(\mathbf{x}), \quad \mathbf{x}(0) = \mathbf{x}_0 \tag{3.1}$$

admit an equilibrium state $\mathbf{x}^* \in \mathbb{R}^n$, i.e. $\mathbf{f}(\mathbf{x}^*) = \mathbf{0}$. We assume that the mapping $\mathbf{f}(\cdot)$ is continuously differentiable in a neighborhood of $\mathbf{x}^*$.

The X-factorable transformation of (3.1) is a similarity transformation in the form:

$$\Sigma : \ \dot{\mathbf{x}} = \mathbf{f}(\mathbf{x}) \quad \rightarrow \quad \Sigma_T : \ \dot{\mathbf{x}} = \mathbf{x} \circ \mathbf{f}(\mathbf{x} - \mathbf{c}), \tag{3.2}$$

where $\mathbf{c} = (c_i)\mathbb{R}^n_{>0}$ is a vector of constant state shift. The above transformation includes a shifting and a multiplying step.

Dynamic equivalence. In the paper [36], the authors affirm that if the strictly positive fixed point of the transformed system satisfies $\mathbf{x}^* + \mathbf{c}^* >> \mathbf{0}$, then the transformed system is dynamically equivalent to the original system, i.e. the local stability of the original system around the equilibrium point yields to the local stability of the transformed system around the shifted equilibrium point and vice versa.

However, this statement is generally not true.

First, it is straightforward to construct simple examples showing that the stability of the original system does not necessarily coincide with that of its transformed counterpart.

Example: Let the linear system and its transformed form be as follows:

$$\Sigma : \ \dot{\mathbf{x}} = A\mathbf{x} \quad \rightarrow \quad \Sigma_T : \ \dot{\mathbf{x}} = \mathbf{x} \circ A(\mathbf{x} - \mathbf{c}) \tag{3.3}$$

such that

$$A = \begin{pmatrix} -0.65999503 & 0.19769598 \\ -1.54726399 & 0.18568017 \end{pmatrix}, \qquad \mathbf{c} = \begin{pmatrix} 1.13861382 \\ 9.54937552 \end{pmatrix}.$$

The eigenvalues of the matrix A are

$$\lambda(A) \approx -0.23715743 \pm 0.35650558\, i.$$

The Jacobian of the transformed system Σ_T is:

$$Df_T = \operatorname{diag}\left(A(\mathbf{x} - \mathbf{c})\right) + \operatorname{diag}\left(\mathbf{x}\right) A. \tag{3.4}$$

The eigenvalues of the transformed system's Jacobian in the equilibrium point $\mathbf{x} = \mathbf{c}$ are

$$\lambda(\operatorname{diag}(\mathbf{c})A) \approx 0.51082513 \pm 1.31625281\, i.$$

Hence, the transformed system Σ_T does not preserve the stability of the original system Σ.

Moreover, such a counterexample is presented in [39], which shows that the dynamical equivalence cannot be guaranteed, even for arbitrarily large state shifts $\mathbf{c}$.

Motivated by these facts, we seek to identify additional conditions under which stability is preserved by the X-factorable transformation.

Definition 1. *(Local diagonal stability) The continuously differentiable mapping* $\mathbf{f}(\cdot)$ *in* (3.1) *is locally diagonally stable in* $\mathbf{x}^*$ *if* $\exists\ \Lambda = \text{diag}\,(\lambda_i)$, $\lambda_i > 0$ *such that*

$$\Lambda\, Df(\mathbf{x}^*) + Df(\mathbf{x}^*)^T \Lambda < 0, \tag{3.5}$$

where Df *is the Jacobian of* $\mathbf{f}(\cdot)$.

Note that the above definition is a generalization of the diagonal stability condition in Eq. (2.7).

Lemma 1. *The mapping* $\mathbf{f}(\mathbf{x})$ *is locally diagonally stable in* $\mathbf{x}^*$ *where* $\mathbf{f}(\mathbf{x}^*) = \mathbf{0}$ *if and only if the mapping* $\mathbf{f}_T(\mathbf{x}) = \mathbf{x} \circ \mathbf{f}(\mathbf{x} - \mathbf{c})$ *is locally diagonally stable in* $\mathbf{x}^{**} = \mathbf{x}^* + \mathbf{c}$ *where* $\mathbf{x}^* + \mathbf{c} \geq \mathbf{0}$.

Proof If Df is the Jacobian of $\mathbf{f}(\mathbf{x})$, then the Jacobian of $\mathbf{f}_T(\mathbf{x})$ is:

$$Df_T(\mathbf{x}) = \text{diag}\,(\mathbf{f}(\mathbf{x} - \mathbf{c})) + \text{diag}\,(\mathbf{x})\, Df(\mathbf{x} - \mathbf{c}). \tag{3.6}$$

It yields

$$Df_T(\mathbf{x}^* + \mathbf{c}) = \text{diag}\,(\mathbf{x}^* + \mathbf{c})\, Df(\mathbf{x}^*). \tag{3.7}$$

Now, we recall the general fact that if a square matrix M is diagonally stable, i.e. it satisfies (2.7), then diag($\mathbf{c}$) M is also diagonally stable for arbitrary $\mathbf{c} > \mathbf{0}$.

Since $\mathbf{x}^* + \mathbf{c} > \mathbf{0}$, if $Df(\mathbf{x}^*)$ is diagonally stable, then $Df(\mathbf{x}^* + \mathbf{c})$ is diagonally stable and vice versa. □

The lemma above can be seen as a generalization of the Lyapunov-type stability condition of the LV system, see e.g. [20]. The Lotka-Volterra system $\dot{\mathbf{x}} = \mathbf{x} \circ M(\mathbf{x} - \mathbf{c})$ is locally asymptotically stable in its equilibrium point if its coefficient matrix M is diagonally stable. This implies that the "underlying" linear system $\dot{\mathbf{x}} = M\mathbf{x}$ is also asymptotically stable. It should be noted that the affirmation of the lemma is valid only locally, in the neighborhood of the equilibrium points.

Diagonal stability of a matrix implies Hurwitz stability, since the existence of a positive definite diagonal Lyapunov function ensures that all eigenvalues have negative real parts. However, the converse is not generally true: A Hurwitz stable matrix need not be diagonally stable [40].

4. Quasi-polynomial model of transformed Lotka-Volterra networks

4.1. X-factorable transformation of Lotka-Volterra networks

To facilitate the control design, the interconnected patch model (2.17) will be transformed into a quasi-polynomial form by applying the X-factorable transformation.

First, consider the *shifted form of the Lotka-Volterra subsystems*:

$$\dot{\mathbf{x}}^{(j)} = (\mathbf{x}^{(j)} - \mathbf{c}^{(j)}) \circ \left(M^{(j)} \left(\mathbf{x}^{(j)} - \mathbf{c}^{(j)} \right) + \mathbf{r}^{(j)} - \mathbf{b}^{(j)} \right) + \sum_{i \in \mathcal{N}_I^{(j)}} \alpha_{ij} \mathbf{b}^{(i)} \circ \left(\mathbf{x}^{(i)} - \mathbf{c}^{(j)} \right).$$

The vector $\mathbf{c} = \left(\mathbf{c}^{(j)T} \right)^T$ is a fixed point of the global model of the shifted interconnected system.

In view of (3.2), the final form of the *transformed subsystem* yields in a *QP form*

$$\dot{\mathbf{x}}^{(j)} = \mathbf{x}^{(j)} \circ \left(M^{(j)} \left(\mathbf{x}^{(j)} - \mathbf{c}^{(j)} \right) \circ \left(\mathbf{x}^{(j)} - \mathbf{c}^{(j)} \right) + \left(\mathbf{r}^{(j)} - \mathbf{b}^{(j)} \right) \circ \left(\mathbf{x}^{(j)} - \mathbf{c}^{(i)} \right) + \sum_{i \in \mathcal{N}_I^{(j)}} \alpha_{ij} \mathbf{b}^{(i)} \circ \left(\mathbf{x}^{(i)} - \mathbf{c}^{(i)} \right) \right). \quad (4.1)$$

Note that the resulting model belongs to the class of second-order Lotka–Volterra systems, as defined in (2.8), and therefore it is a QP system of special form.

Example 2. *The X-transformed version of the state equations from Example 1 reads as:*

$$\begin{pmatrix} \dot{x}_1^{(1)} \\ \dot{x}_2^{(1)} \end{pmatrix} = \begin{pmatrix} x_1^{(1)} \\ x_2^{(1)} \end{pmatrix} \circ \left(\begin{bmatrix} m_{11}^{(1)} & m_{12}^{(1)} & 0 \\ 0 & m_{21}^{(1)} & m_{22}^{(1)} \end{bmatrix} \begin{pmatrix} (x_1^{(1)} - c_1^{(1)})^2 \\ (x_1^{(1)} - c_1^{(1)})(x_2^{(1)} - c_2^{(1)}) \\ (x_2^{(1)} - c_2^{(1)})^2 \end{pmatrix} + \begin{pmatrix} r_1^{(1)} - \beta_1 \\ r_2^{(1)} - \beta_1 \end{pmatrix} \circ \begin{pmatrix} x_1^{(1)} - c_1^{(1)} \\ x_2^{(1)} - c_2^{(1)} \end{pmatrix} + \beta_2 \begin{pmatrix} x_1^{(2)} - c_1^{(2)} \\ x_2^{(2)} - c_2^{(2)} \end{pmatrix} \right), \quad (4.2)$$

$$\begin{pmatrix} \dot{x}_1^{(2)} \\ \dot{x}_2^{(2)} \end{pmatrix} = \begin{pmatrix} x_1^{(2)} \\ x_2^{(2)} \end{pmatrix} \circ \left(\begin{bmatrix} m_{11}^{(2)} & m_{12}^{(2)} & 0 \\ 0 & m_{21}^{(2)} & m_{22}^{(2)} \end{bmatrix} \begin{pmatrix} (x_1^{(2)} - c_1^{(2)})^2 \\ (x_1^{(2)} - c_1^{(2)})(x_2^{(2)} - c_2^{(2)}) \\ (x_2^{(2)} - c_2^{(2)})^2 \end{pmatrix} + \begin{pmatrix} r_1^{(2)} - \beta_2 \\ r_2^{(2)} - \beta_2 \end{pmatrix} \circ \begin{pmatrix} x_1^{(2)} - c_1^{(2)} \\ x_2^{(2)} - c_2^{(2)} \end{pmatrix} + \beta_1 \begin{pmatrix} x_1^{(1)} - c_1^{(1)} \\ x_2^{(1)} - c_2^{(1)} \end{pmatrix} \right). \quad (4.3)$$

In order to obtain an *approximate decoupled model* of the interconnected system, the transformation (2.24), originally defined for relating the equilibrium states, will be applied to the time-varying states as follows:

$$\mathbf{x}^{(i)} - \mathbf{c}^{(i)} = \mathbf{t}_{ij} \circ (\mathbf{x}^{(j)} - \mathbf{c}^{(j)}) + \boldsymbol{d}_{ij}. \quad (4.4)$$

Here $\boldsymbol{d}_{ij} \in \mathbb{R}^m$ is the time-dependent additive approximation error.

The approximate decoupled model is

$$\dot{\mathbf{x}}^{(j)} = \mathbf{x}^{(j)} \circ \left(M^{(j)} \left(\mathbf{x}^{(j)} - \mathbf{c}^{(j)} \right) \circ \left(\mathbf{x}^{(j)} - \mathbf{c}^{(j)} \right) + \underbrace{\left(\mathbf{r}^{(j)} - \mathbf{b}^{(j)} + \sum_{i \in \mathcal{N}_I^{(j)}} \alpha_{ij} \mathbf{b}^{(i)} \circ \mathbf{t}_{ij} \right)}_{\boldsymbol{\rho}^{(j)}} \circ \left(\mathbf{x}^{(j)} - \mathbf{c}^{(j)} \right) + \boldsymbol{\delta}^{(j)} \right), \quad (4.5)$$

where the cumulative approximation error in the jth patch model is

$$\boldsymbol{\delta}^{(j)} = \sum_{i \in \mathcal{N}_I^{(j)}} \alpha_{ij} \mathbf{b}^{(i)} \circ \boldsymbol{\delta}_{ij}. \quad (4.6)$$

Example 3. *The approximate form of the first decoupled subsystem from Example 2 reads as:*

$$\begin{pmatrix} \dot{x}_1^{(1)} \\ \dot{x}_2^{(1)} \end{pmatrix} = \begin{pmatrix} x_1^{(1)} \\ x_2^{(1)} \end{pmatrix} \circ \left(\begin{bmatrix} m_{11}^{(1)} & m_{12}^{(1)} & 0 \\ 0 & m_{21}^{(1)} & m_{22}^{(1)} \end{bmatrix} \begin{pmatrix} (x_1^{(1)} - c_1^{(1)})^2 \\ (x_1^{(1)} - c_1^{(1)})(x_2^{(1)} - c_2^{(1)}) \\ (x_2^{(1)} - c_2^{(1)})^2 \end{pmatrix} + \begin{pmatrix} \rho_1^{(1)} \\ \rho_2^{(1)} \end{pmatrix} \circ \begin{pmatrix} x_1^{(1)} - c_1^{(1)} \\ x_2^{(1)} - c_2^{(1)} \end{pmatrix} + \begin{pmatrix} \delta_1^{(1)} \\ \delta_2^{(1)} \end{pmatrix} \right). \quad (4.7)$$

4.2. QP embedding of the subsystems

As shown in subsection 2.3, a quasi-polynomial model admits an embedding into a Lotka–Volterra model when its state variables are expressed as monomials $\mathbf{q}^{(j)}$. Here, we build on this result by examining the transformed QP model (4.1), focusing on the case where $\mathbf{c}^{(j)} = \mathbf{0}$.

We identify the vector of quasi-monomials $\mathbf{q}^{(j)}$ in Eq. (4.5) that consists of two blocks: (i) a block $\mathbf{q}_2^{(j)}$ of the 2nd order terms $x_i^{(j)} x_k^{(j)}, i, k = 1, ..., m$, and (ii) a block $\mathbf{q}_1^{(j)}$ of the real state variables $x_i^{(j)}, i, = 1, ..., m$.

$$\mathbf{q}^{(j)} = \left[(\mathbf{q}_2^{(j)})^T \;\; \mathbf{q}_1^{(j)})^T \right]^T \in \mathbb{R}^p, \tag{4.8}$$

where the number of quasi-monomials is $p = 2m + \frac{m(m-1)}{2}$.

Then, the interaction and exponent matrices of the QP model are

$$\mathcal{A}^{(j)} = \left[\begin{array}{cc} \overline{M}^{(j)} & \text{diag}(\boldsymbol{\rho}^{(j)}) + \overline{L}^{(j)} \end{array} \right] \in \mathbb{R}^{m \times p} \;\; , \;\; \mathcal{B}^{(j)} = \left[\begin{array}{cccccc} 2 & 0 & 0 & ... & 0 & 0 \\ 1 & 1 & 0 & ... & 0 & 0 \\ 0 & 2 & 0 & ... & 0 & 0 \\ 0 & 0 & 2 & ... & 0 & 0 \\ 0 & 1 & 1 & ... & 0 & 0 \\ 1 & 0 & 1 & ... & 0 & 0 \\ ... & ... & ... & ... & ... & ... \\ 1 & 0 & 0 & ... & 0 & 0 \\ 0 & 1 & 0 & ... & 0 & 0 \\ 0 & 0 & 1 & ... & 0 & 0 \\ ... & ... & ... & ... & ... & ... \\ 0 & 0 & 0 & ... & 0 & 1 \end{array} \right] \in \mathbb{R}^{p \times m}, \tag{4.9}$$

where $\overline{M}^{(j)}$ is computed from the interaction matrix $M^{(j)}$ following the order of the 2nd order terms in (4.8); $\overline{L}^{(j)}$ depends on the interconnection structure.

With the above QP model matrices, one can easily compute the LV form of the subsystem models using (2.10). The LV model parameters are

$$\mathcal{M}^{(j)} = \mathcal{B}^{(j)} \mathcal{A}^{(j)} \;\; , \;\; \boldsymbol{\delta}_{QP}^{(j)} = \mathcal{B}^{(j)} \boldsymbol{\delta}^{(j)}. \tag{4.10}$$

Example 4. *Without applying the approximation, the transformed quasi-monomial vector for the previous Example 2 is*

$$\mathbf{q}(\mathbf{x}) = [(x_1^{(1)})^2 \;\; x_1^{(1)} x_2^{(1)} \;\; (x_2^{(1)})^2 \;\; (x_1^{(2)})^2 \;\; x_1^{(2)} x_2^{(2)} \;\; (x_2^{(2)})^2 \;\; x_1^{(1)} \;\; x_2^{(1)} \;\; x_1^{(2)} \;\; x_2^{(2)}]^T. \tag{4.11}$$

The interaction matrix of the QP model is

$$\mathcal{A} = \left[\begin{array}{cccccccccc} m_{11}^{(1)} & m_{12}^{(1)} & 0 & 0 & 0 & 0 & r_1^{(1)} - \beta_1 & 0 & \beta_2 & 0 \\ 0 & m_{21}^{(1)} & m_{22}^{(1)} & 0 & 0 & 0 & 0 & r_2^{(1)} - \beta_1 & 0 & \beta_2 \\ 0 & 0 & 0 & m_{11}^{(2)} & m_{12}^{(2)} & 0 & \beta_1 & 0 & r_1^{(2)} - \beta_2 & 0 \\ 0 & 0 & 0 & 0 & m_{21}^{(2)} & m_{22}^{(2)} & 0 & \beta_1 & 0 & r_2^{(2)} - \beta_2 \end{array} \right], \tag{4.12}$$

and its exponent matrix is

$$\mathcal{B} = \begin{bmatrix} 2 & 0 & 0 & 0 \\ 1 & 1 & 0 & 0 \\ 0 & 2 & 0 & 0 \\ 0 & 0 & 2 & 0 \\ 0 & 0 & 1 & 1 \\ 0 & 0 & 0 & 2 \\ 1 & 0 & 0 & 0 \\ 0 & 1 & 0 & 0 \\ 0 & 0 & 1 & 0 \\ 0 & 0 & 0 & 1 \end{bmatrix}. \tag{4.13}$$

When $\mathbf{c}^{(j)} \neq \mathbf{0}$, the exponent matrix retains the same structure, while the interaction matrix requires additional terms that depend on the entries of $\mathbf{c}^{(j)}$.

4.3. Extended model with dynamic interconnections

4.3.1. Dynamic connecting pseudo-patches

Single species case. Let us consider two patches indexed by j and i that are connected by a dynamic population size-driven migration channel where the ℓth species $x_\ell^{(i)}$ can migrate from the ith patch to the jth. Let us divide the interconnection channel into p uniform sub-patches, within which the migration is also population size-driven with the uniform flow rate $v_\ell^{(ij)}$.

We model the migration by spatially discretizing the partial differential equation describing the convective transport. Let us denote the population size vector of the ℓth specie, in the interconnecting patch from i to j by $z_\ell^{(ij)}$. The population dynamics in the interconnecting patch is given by the LTI (linear time-invariant) model, similar to that in [41]:

$$\dot{\mathbf{z}}_\ell^{(ij)} = A_\ell^{(ij)}\mathbf{z}_\ell^{(ij)} + B_\ell^{(ij)}\mathbf{u}_\ell^{(ij)}\ , \quad \mathbf{y}^{(ij)} = C\mathbf{z}_\ell^{(ij)}, \tag{4.14}$$

$$\mathbf{z}_\ell^{(ij)} = [z_{\ell 1}^{(ij)}\ z_{\ell 2}^{(ij)}\ \dots\ z_{\ell p}^{(ij)}]^T \in \mathbb{R}^p\ , \quad \mathbf{u}^{(ij)} = x_\ell^{(i)}\ , \quad \mathbf{y}^{(ij)} = z_{\ell p}^{(ij)}, \tag{4.15}$$

where

$$A_\ell^{(ij)} = \begin{bmatrix} -v_\ell^{(ij)} & 0 & 0 & ... & 0 & 0 & 0 \\ v_\ell^{(ij)} & -v_\ell^{(ij)} & 0 & ... & 0 & 0 & 0 \\ 0 & v_\ell^{(ij)} & -v_\ell^{(ij)} & ... & 0 & 0 & 0 \\ ... & ... & ... & ... & ... & ... & ... \\ 0 & 0 & 0 & ... & v_\ell^{(ij)} & -v_\ell^{(ij)} & 0 \\ 0 & 0 & 0 & ... & 0 & v_\ell^{(ij)} & -v_\ell^{(ij)} \end{bmatrix}, \tag{4.16}$$

$$C_\ell^{(ij)} = \begin{bmatrix} 0 & 0 & 0 & ... & 1 \end{bmatrix}\ , \quad B_\ell^{(ij)} = \begin{bmatrix} v_\ell^{(ij)} \\ 0 \\ ... \\ 0 \end{bmatrix}. \tag{4.17}$$

Note that this pseudo-patch has a population size-driven (one-directional) connection with its two neighbors, patches i and j, but describes only the ℓth species.

Multiple species case. We can generalize the above single species case for multiple species $\ell = 1, ..., m$ by constructing the following composite state, input, and output vectors:

$$\begin{aligned} &\mathbf{z}^{(ij)} = [\mathbf{z}_1^{(ij)T}\ \mathbf{z}_2^{(ij)T}\ \ \dots\ \mathbf{z}_m^{(ij)T}]^T \in \mathbb{R}^{mp}, \\ &\mathbf{u}^{(ij)} = \mathbf{x}^{(i)} \in \mathbb{R}^m\ ,\ \ \mathbf{y}^{(jk)} = [z_{1p}^{(ij)}\ ...\ z_{1p}^{(ij)}\ \ \dots\ z_{mp}^{(ij)}]^T \in \mathbb{R}^m, \end{aligned} \tag{4.18}$$

with the following coefficient matrices:

$$A^{(ij)} = \begin{bmatrix} A_1^{(ij)} & O & ... & O & O \\ O & A_2^{(ij)} & ... & O & O \\ ... & ... & ... & ... & ... \\ O & O & ... & A_{m-1}^{(ij)} & O \\ O & O & ... & O & A_m^{(ij)} \end{bmatrix} \in \mathbb{R}^{mp\times mp}, \tag{4.19}$$

$$C^{(ij)} = \begin{bmatrix} C_1^{(ij)} & O & ... & O \\ O & C_2^{(ij)} & ... & O \\ ... & ... & ... & ... \\ O & O & ... & C_m^{(ij)} \end{bmatrix} \in \mathbb{R}^{m\times(pm)}\ ,\ B^{(ij)} = \begin{bmatrix} B_1^{(ij)} & O & ... & O \\ O & B_2^{(ij)} & ... & O \\ ... & ... & ... & ... \\ O & O & ... & B_m^{(ij)} \end{bmatrix} \in \mathbb{R}^{(mp)\times m}. \tag{4.20}$$

With the above vectors and matrices, the following LTI model is obtained for the dynamic connecting pseudo-patches:

$$\dot{\mathbf{z}}^{(ij)} = A^{(ij)}\mathbf{z}^{(ij)} + B^{(ij)}\mathbf{x}^{(i)}\ ,\ \ \mathbf{y}^{(ij)} = C^{(ij)}\mathbf{z}^{(ij)}. \tag{4.21}$$

Note that the $\mathbf{y}^{(ij)}$ output vector serves to connect the dynamic connecting pseudo-patch to the destination LV patch.

With dynamic connecting elements at its inputs, the subsystem models (2.17) can be extended as:

$$\begin{aligned} \dot{\mathbf{x}}^{(j)} &= \mathbf{x}^{(j)} \circ \left(M^{(j)}\mathbf{x}^{(j)} + \mathbf{r}^{(j)}\right) - \mathbf{b}^{(j)} \circ \mathbf{x}^{(j)} + \sum_{i\in\mathcal{N}_I^{(j)}} C^{(ij)}\mathbf{z}^{(ij)}, \\ \dot{\mathbf{z}}^{(ij)} &= A^{(ij)}\mathbf{z}^{(ij)} + B^{(ij)}\alpha_{ij}\mathbf{b}^{(i)} \circ \mathbf{x}^{(i)}, \quad i = 1 \dots \dim(\mathcal{N}_I^{(j)}). \end{aligned} \tag{4.22}$$

4.3.2. Embedding the dynamic connecting pseudo-patches

As it was presented in subsection 4.3.1, the dynamic (i.e., delayed) interconnections can be (approximately) realized by positive linear compartmental subsystems that have an LTI model of the form (4.21). So, we may use the QP-embedding of such subsystems to form a homogeneous QP-model of the networked LV model with delayed interconnections.

For this purpose, we use the X-factorable transformation (3.2) to extend the transformed model (4.1) with dynamic connections:

$$\dot{\mathbf{x}}^{(j)} = \mathbf{x}^{(j)} \circ \left(M^{(j)} \left(\mathbf{x}^{(j)} - \mathbf{c}^{(j)}\right) \circ \left(\mathbf{x}^{(j)} - \mathbf{c}^{(j)}\right) + \left(\mathbf{r}^{(j)} - \mathbf{b}^{(j)}\right) \circ \left(\mathbf{x}^{(j)} - \mathbf{c}^{(j)}\right) + \sum_{i\in\mathcal{N}_I^{(j)}} \mathbf{z}^{(ij)} \right) \tag{4.23}$$

$$\dot{\mathbf{z}}^{(ij)} = \mathbf{z}^{(ij)} \circ \left(A^{(ij)}\mathbf{z}^{(ij)} + B^{(ij)}\alpha_{ij}\mathbf{b}^{(i)} \circ (\mathbf{x}^{(i)} - \mathbf{c}^{(i)})\right), \quad i = 1 \dots \dim(\mathcal{N}_I^{(j)}) \tag{4.24}$$

It was applied that the steady state gain of system (4.14) is 1.

Therefore, a networked LV system with delays will have dynamic LV and LTI nodes and linear connections, which can also be embedded into a QP-form.

Example 5. *Let us consider the same system described in Example 2 but extended with dynamic migration channels (see in subsection 4.3.1). This is a network of two 2-dimensional Lotka-Volterra systems that are interconnected by a bidirectional migration channel, described in Eqs* (2.22)-(2.23)*, that is now extended by two dynamic pseudo-patches described in Eqs.* (4.21) *with 3 sub-patches (i.e.* $p = 3$*,* $\ell = 1, 2$*). For the sake of simplicity we assume uniform flow rates* $v_\ell^{(ij)} = v$*;* $i, j = 1, 2,\ \ell = 1, 2$*.*

The block diagram of the interconnected system is presented in Figure 1.

Then, the X-factorable transformed versions of the state equations for the four patches (two LV patches and two delayed pseudo-patches) without approximation are as follows:

$$\begin{pmatrix} \dot{x}_1^{(1)} \\ \dot{x}_2^{(1)} \end{pmatrix} = \begin{pmatrix} x_1^{(1)} \\ x_2^{(1)} \end{pmatrix} \circ \left(\begin{bmatrix} m_{11}^{(1)} & m_{12}^{(1)} & 0 \\ 0 & m_{21}^{(1)} & m_{22}^{(1)} \end{bmatrix} \begin{pmatrix} (x_1^{(1)} - c_1^{(1)})^2 \\ (x_1^{(1)} - c_1^{(1)})(x_2^{(1)} - c_2^{(1)}) \\ (x_1^{(1)} - c_2^{(1)})^2 \end{pmatrix} + \begin{pmatrix} r_1^{(1)} - \beta_1 \\ r_2^{(1)} - \beta_1 \end{pmatrix} \circ \begin{pmatrix} (x_1^{(1)} - c_1^{(1)}) \\ (x_2^{(1)} - c_2^{(1)}) \end{pmatrix} + \beta_2 \begin{pmatrix} z_{13}^{(21)} \\ z_{23}^{(21)} \end{pmatrix} \right), \tag{4.25}$$

$$\begin{pmatrix} \dot{x}_1^{(2)} \\ \dot{x}_2^{(2)} \end{pmatrix} = \begin{pmatrix} x_2^{(2)} \\ x_2^{(2)} \end{pmatrix} \circ \left(\begin{bmatrix} m_{11}^{(2)} & m_{12}^{(2)} & 0 \\ 0 & m_{21}^{(2)} & m_{22}^{(2)} \end{bmatrix} \begin{pmatrix} (x_1^{(2)} - c_1^{(2)})^2 \\ (x_1^{(2)} - c_1^{(2)})(x_2^{(2)} - c_2^{(2)}) \\ (x_2^{(2)} - c_2^{(2)})^2 \end{pmatrix} + \begin{pmatrix} r_1^{(2)} - \beta_2 \\ r_2^{(2)} - \beta_2 \end{pmatrix} \circ \begin{pmatrix} (x_1^{(2)} - c_1^{(2)}) \\ (x_2^{(2)} - c_2^{(2)}) \end{pmatrix} + \beta_1 \begin{pmatrix} z_{13}^{(12)} \\ z_{23}^{(12)} \end{pmatrix} \right), \tag{4.26}$$

$$\begin{pmatrix} \dot{z}_{11}^{(12)} \\ \dot{z}_{12}^{(12)} \\ \dot{z}_{13}^{(12)} \\ \dot{z}_{21}^{(12)} \\ \dot{z}_{22}^{(12)} \\ \dot{z}_{23}^{(12)} \end{pmatrix} = \begin{pmatrix} z_{11}^{(12)} \\ z_{12}^{(12)} \\ z_{13}^{(12)} \\ z_{21}^{(12)} \\ z_{22}^{(12)} \\ z_{23}^{(12)} \end{pmatrix} \circ \left(\begin{bmatrix} -v & 0 & 0 & 0 & 0 & 0 \\ v & -v & 0 & 0 & 0 & 0 \\ 0 & v & -v & 0 & 0 & 0 \\ 0 & 0 & v & -v & 0 & 0 \\ 0 & 0 & 0 & v & -v & 0 \\ 0 & 0 & 0 & 0 & v & -v \end{bmatrix} \begin{pmatrix} z_{11}^{(12)} \\ z_{12}^{(12)} \\ z_{13}^{(12)} \\ z_{21}^{(12)} \\ z_{22}^{(12)} \\ z_{23}^{(12)} \end{pmatrix} + v\beta_1 \begin{pmatrix} x_1^{(1)} - c_1^{(1)} \\ 0 \\ 0 \\ x_2^{(1)} - c_2^{(1)} \\ 0 \\ 0 \end{pmatrix} \right) \tag{4.27}$$

$$\begin{pmatrix} \dot{z}_{11}^{(21)} \\ \dot{z}_{12}^{(21)} \\ \dot{z}_{13}^{(21)} \\ \dot{z}_{21}^{(21)} \\ \dot{z}_{22}^{(21)} \\ \dot{z}_{23}^{(21)} \end{pmatrix} = \begin{pmatrix} z_{11}^{(21)} \\ z_{12}^{(21)} \\ z_{13}^{(21)} \\ z_{21}^{(21)} \\ z_{22}^{(21)} \\ z_{23}^{(21)} \end{pmatrix} \circ \left(\begin{bmatrix} -v & 0 & 0 & 0 & 0 & 0 \\ v & -v & 0 & 0 & 0 & 0 \\ 0 & v & -v & 0 & 0 & 0 \\ 0 & 0 & v & -v & 0 & 0 \\ 0 & 0 & 0 & v & -v & 0 \\ 0 & 0 & 0 & 0 & v & -v \end{bmatrix} \begin{pmatrix} z_{11}^{(21)} \\ z_{12}^{(21)} \\ z_{13}^{(21)} \\ z_{21}^{(21)} \\ z_{22}^{(21)} \\ z_{23}^{(21)} \end{pmatrix} + v\beta_2 \begin{pmatrix} x_1^{(2)} - c_1^{(2)} \\ 0 \\ 0 \\ x_2^{(2)} - c_2^{(2)} \\ 0 \\ 0 \end{pmatrix} \right). \tag{4.28}$$

5. Setpoint control based on the transformed model

As discussed in section 2, population persistence can be guaranteed if the subsystem possesses an asymptotically stable and strictly positive equilibrium state. To achieve this, a feedback control strategy is proposed in this section to shift the potentially nonpositive equilibria toward a strictly positive setpoint and to maintain the attractiveness of these equilibria despite modeling uncertainties.

Consider the original system (2.12) extended with a control input $\mathbf{u}^{(j)}$ as

$$\dot{\mathbf{x}}^{(j)} = \mathbf{x}^{(j)} \circ \left(M^{(j)} \mathbf{x}^{(j)} + \mathbf{r}^{(j)} \right) - \mathbf{v}_O^{(j)} + \mathbf{v}_I^{(j)} + B_c^{(j)} \mathbf{u}^{(j)}, \tag{5.1}$$

where $B_c^{(j)}$ is a control input matrix such that $B_c^{(j)} B_c^{(j)+} = I$.

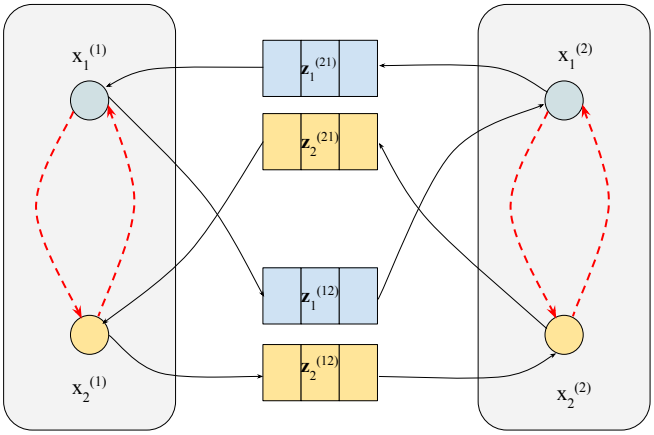

Figure 1. Two Lotka-Volterra systems with dynamic interconnections.

This control input can be viewed as the population settling- or relocation rate. When its sign is positive, population settling has to be implemented with a given rate. Otherwise, population relocation has to be performed. It should be noted that population settling can be implemented physically by adding species to a patch from an external source, while population relocation can be performed by harvesting and removing species from a patch, if possible.

Control problem. Let $\mathbf{x}_{SP}^{(j)} \in \mathbb{R}_{>0}^{m}$ be the setpoint (prescribed state vector) for the jth subsystem. Design the feedback control $\mathbf{u}^{(j)} = \mathbf{u}^{(j)}(\mathbf{x}^{(j)})$ such that $\lim_{t\to\infty} \|\mathbf{x}_{SP}^{(j)} - \mathbf{x}^{(j)}(t)\| < \epsilon(\delta)$, where $\epsilon(\delta) > 0$ is an uncertainty magnitude-dependent precision.

To design the control input, the transformed system model (4.5) is applied. In this case, instead of an arbitrary state shift, let $\mathbf{c}^{(i)} = \mathbf{x}_{SP}^{(i)}$. The transformed model with control reads as

$$\dot{\mathbf{x}}^{(j)} = \mathbf{x}^{(j)} \circ \left(M^{(j)} \left(\mathbf{x}^{(j)} - \mathbf{x}_{SP}^{(j)} \right) \circ \left(\mathbf{x}^{(j)} - \mathbf{x}_{SP}^{(j)} \right) + \boldsymbol{\rho}^{(j)} \circ \left(\mathbf{x}^{(j)} - \mathbf{x}_{SP}^{(j)} \right) + \boldsymbol{\delta}^{(j)} + B_c^{(j)} \mathbf{u} \right). \tag{5.2}$$

The setpoint $\mathbf{x}_{SP}^{(j)}$ is an equilibrium state of the system when the modeling uncertainties and the control are omitted. The feedback control has to be designed such that

- it introduces additional stabilizer terms into the model when the dynamics of the system around the equilibrium $\mathbf{x}_{SP}^{(j)}$ is not attractive, and
- it mitigates the effect of the approximation error $\boldsymbol{\delta}^{(j)}$ on tracking performance.

The linearized system model around $\mathbf{x}_{SP}^{(j)}$ has the form:

$$\dot{\mathbf{e}}^{(j)} = \mathbf{e}^{(j)} \circ \left(\mathbf{x}_{SP}^{(j)} \circ \boldsymbol{\rho}^{(j)} + \boldsymbol{\delta}^{(j)} + B_c^{(j)} \mathbf{u}^{(j)} \right), \tag{5.3}$$

where $\mathbf{e}^{(j)} = \mathbf{x}^{(j)} - \mathbf{x}_{SP}^{(j)}$. Note that the second-order terms cancel out due to linearization.

Let the control law be

$$\mathbf{u}^{(j)} = B_c^{(j)+} \left(\mathbf{k}^{(j)} \circ \mathbf{e}^{(j)} - \mathbf{x}_{SP}^{(j)} \circ \boldsymbol{\rho}^{(j)} \right), \tag{5.4}$$

where $\mathbf{k}^{(j)} > \mathbf{0}$ is the control gain vector.

Around the equilibrium point, the linearized dynamics of the controlled system resemble a Lotka–Volterra type system:

$$\dot{\mathbf{e}}^{(j)} = \mathbf{e}^{(j)} \circ \left(\operatorname{diag}\left(\mathbf{k}^{(j)}\right)\mathbf{e}^{(j)} + \boldsymbol{\delta}^{(j)}\right). \tag{5.5}$$

It is important to note that the above proposed numerically simple controller has the following advantageous properties:

- In view of the stability properties presented in section 2, the controlled system is locally diagonally stable around the setpoint $\mathbf{x}_{SP}^{(j)}$.
- Moreover, as noted in [25], larger controller gains improve disturbance attenuation, mitigating the effect of the disturbance offset term on control performance.
- Building on the lemma in section 3, the controller defined in (5.4) guarantees *local stability* of the original controlled nonlinear system around the prescribed setpoint.
- Furthermore, the proposed control strategy can be implemented in a *decentralized* manner: The control input for the jth subsystem depends exclusively on the states of that subsystem.

Controller implementation and computational complexity. The implementation of the controller (5.4) does not require communication among subsystems, relying solely on local measurements. Given $B_c^{(j)+}$, $\mathbf{k}^{(j)}$, $\boldsymbol{\rho}^{(j)}$, and $\mathbf{x}_{SP}^{(j)}$, the control action is a static linear transformation of the measured state vector $\mathbf{x}^{(j)}$. Hence, the controller has a low computational cost.

Moreover, as the controllers are decentralized and their computational complexity is polynomial, the computational cost remains polynomial in the number of Lotka-Volterra subsystems, too. This fact enables the application of the method effectively for ecological systems with a large number of subsystems.

6. Case study

The numerical simulations were carried out to demonstrate and validate the proposed theoretical modeling and control framework.

All experiments were performed in the MATLAB/Simulink environment. The system dynamics were integrated using the `ode45` solver with a maximum integration step of 0.001 and an absolute tolerance of 10^{-4} in both the controlled and uncontrolled scenarios. The simulations were carried out in continuous time using a Level-2 MATLAB S-function implementation of the nonlinear plant, ensuring direct numerical integration of the system dynamics.

The benchmark system consists of two interconnected two-dimensional Lotka–Volterra subsystems introduced in Example 1, resulting in a four-state nonlinear model of the form $[x_1^{(1)}, x_2^{(1)}, x_1^{(2)}, x_2^{(2)}]^\top$. The intra-species interaction matrices were defined as

$$M_1 = M_2 = \begin{bmatrix} 0 & -1 \\ 1 & 0 \end{bmatrix},$$

while the intrinsic growth rate vectors were set to $r_1 = r_2 = [0.3, -0.3]^\top$. The interconnection strengths were chosen as $\beta_1 = 0.01$ and $\beta_2 = 0.5$, introducing an asymmetric coupling between the subsystems. The initial conditions for all states were uniformly selected as $x_i^{(j)}(0) = 0.5$, ensuring operation in the positive orthant.

The control inputs (5.4) were implemented as additive two-dimensional signals acting on each subsystem. A decentralized diagonal feedback structure was employed with uniform controller gains for all input channels.

Three simulation scenarios were investigated.

6.1. Uncontrolled interconnected dynamics

The first simulation analyzed the natural behavior of the interconnected system described by (2.22). The resulting state trajectories are depicted in Figure 2. Consistent with the steady-state analysis presented in Example 1, subsystem 2 experiences population extinction. This behavior arises from the asymmetry in the interconnection terms: The emigration rate from subsystem 2 to subsystem 1 is significantly greater than the reverse flow. After the initial transient response, the dynamics of subsystem 1 resemble those of a classical predator–prey system.

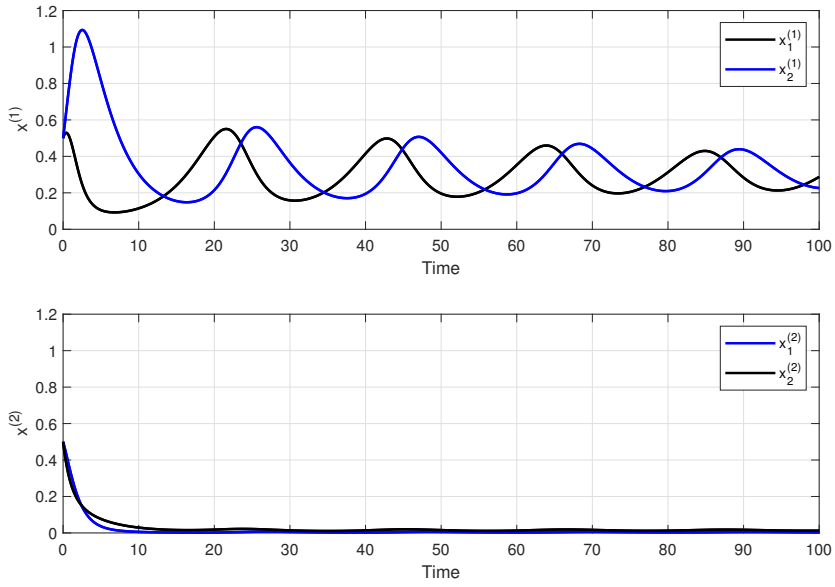

Figure 2. Trajectories of interconnected Lotka-Volterra systems.

6.2. Influence of distributed delay

In the second simulation scenario, the effect of interconnection delays on the system dynamics was examined. The coupling terms were augmented with the delay pseudo-patches introduced in Example 5. The parameters were set to $p = 3$ and $v = 0.1$. As illustrated in Figure 3, the introduction of delay modifies the transient behavior, yet the extinction of subsystem 2 persists, indicating that the qualitative outcomes of the interaction remain unchanged.

Further simulation experiments were conducted to investigate the effect of a time-varying delay. In this case, the coefficients associated with the distributed delay terms were modeled as periodic functions rather than constants, according to $v_{\text{eff}}(t) = v\,(1 + A_v \sin(2\pi f_v t))$, where $A_v = 0.9$ and $f_v = 0.05$ Hz.

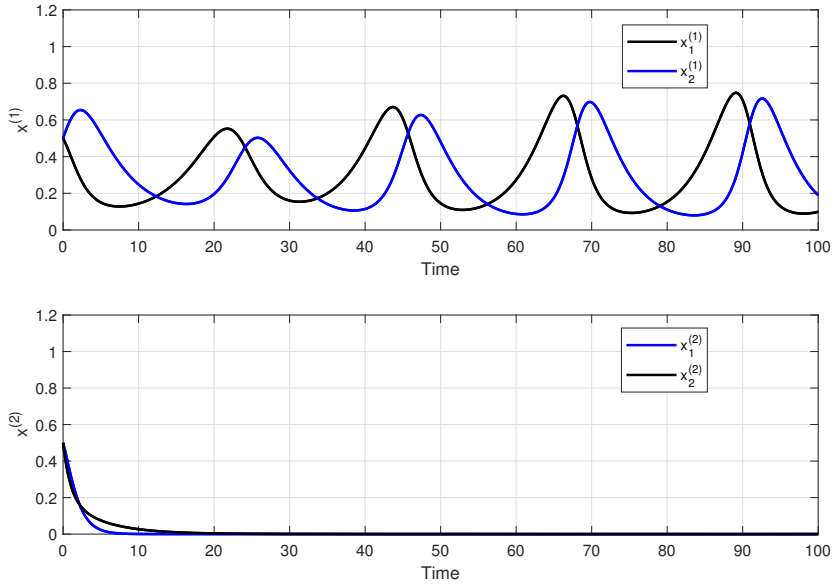

Figure 3. Trajectories of interconnected Lotka-Volterra systems with delay.

In comparison with the constant-delay scenario, it can be observed in Figure 4, that the time-varying nature of the delay significantly influences the transient dynamics. Both the amplitude and the period of the resulting nonlinear oscillatory evolution are modified. However, the qualitative behavior of the system remains unchanged.

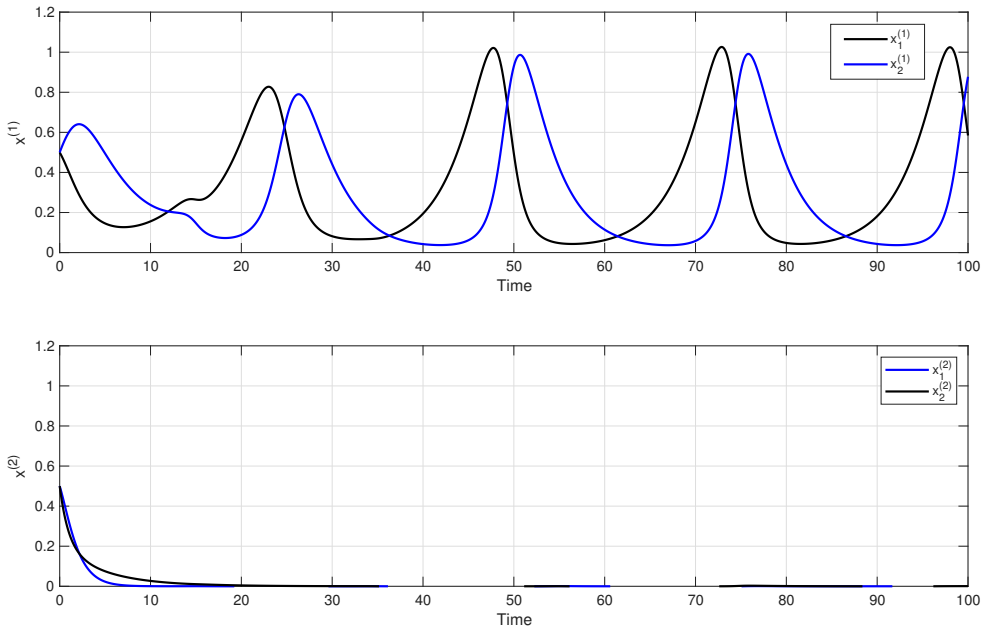

Figure 4. Trajectories of interconnected Lotka-Volterra systems with time-varying delay.

6.3. Controlled interconnected dynamics

The third simulation investigated the closed-loop behavior under the control strategy proposed in section 5. The desired setpoints were selected as

$$x_{\mathrm{SP1}}^{(1)} = 3, \quad x_{\mathrm{SP2}}^{(1)} = 2.5, \quad x_{\mathrm{SP1}}^{(2)} = 1, \quad x_{\mathrm{SP2}}^{(2)} = 0.75.$$

The control law (5.4) was implemented using identical gains in all channels, $k_i^{(j)} = k$ for $i, j = 1, 2$. The input matrix was chosen as the identity matrix. As shown in Figure 5, with $k = 100$, the trajectories converge toward the prescribed setpoints, though small steady-state tracking errors remain due to unmodeled dynamics. Increasing the control gain to $k = 1000$ significantly reduces these errors, confirming the capacity of the proposed controller to deal with modeling uncertainties.

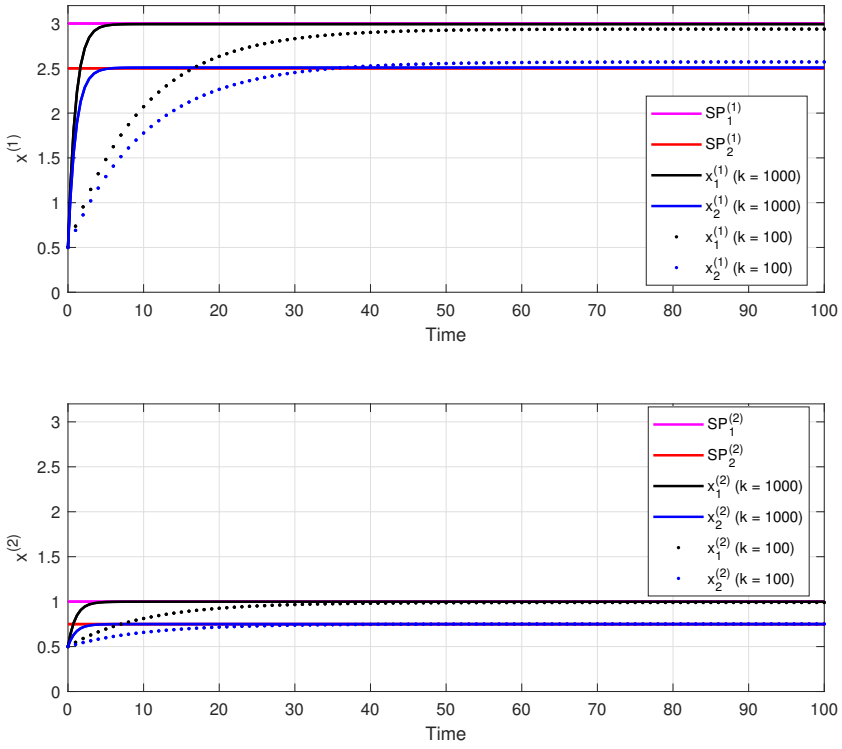

Figure 5. Trajectories of interconnected Lotka-Volterra systems with control.

The control signals are presented in Figure 6. As shown, increasing the control gain results in higher-magnitude control inputs during the transient phase. However, once the system approaches steady state, the required control effort significantly decreases, and only low-magnitude inputs are needed to maintain accurate setpoint tracking.

To evaluate the robustness of the system in the presence of uncertainty, stochastic simulations were also conducted. In this case, the ith state of the jth subsystem in (5.1) was modeled as:

$$dx_i^{(j)} = x_i^{(j)} \left(\left(M^{(j)}\mathbf{x}^{(j)}\right)_i + r_i^{(j)} \right) dt - v_{O,i}^{(j)}\, dt + v_{I,i}^{(j)}\, dt + \left(B_c^{(j)}\mathbf{u}^{(j)}\right)_i dt + x_i^{(j)}\sigma_i^{(j)}\, dW^{(j)}(t). \tag{6.1}$$

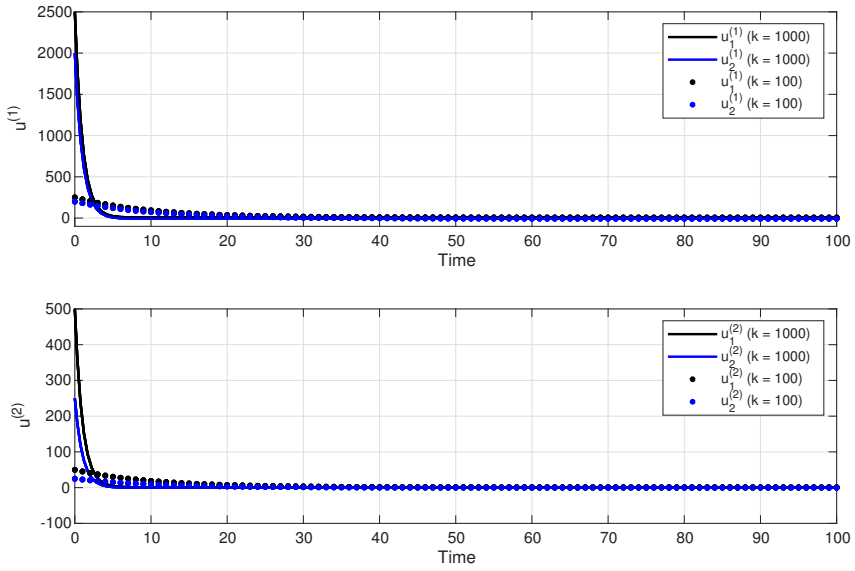

Figure 6. Control signals.

The coefficients $\sigma_i^{(j)}$ determine the intensity of stochastic fluctuations acting on the state components. During the simulations, it was considered that $\sigma_i^{(j)} = 100$, $i, j = 1, 2$. The processes $dW^{(j)}(t)$ are increments of independent standard Wiener processes, satisfying $dW^{(j)}(t) \sim \mathcal{N}(0, dt)$.

The simulation results in Figure 7 show that the controlled interconnected system preserves accurate setpoint tracking performance despite the presence of stochastic disturbances.

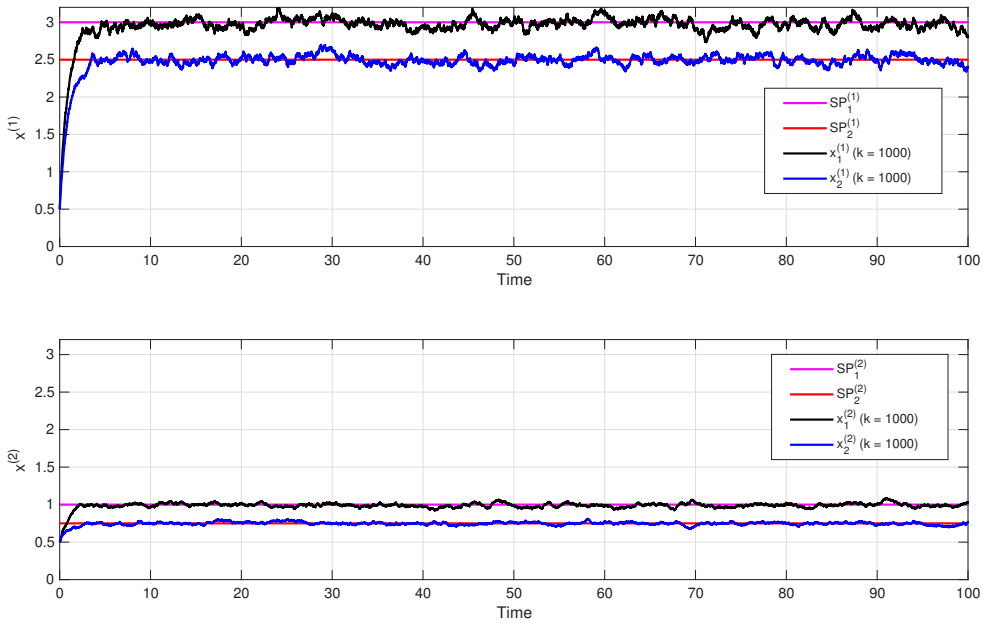

Figure 7. Trajectories of interconnected Lotka-Volterra systems with control and stochastic disturbances.

7. Conclusions

A dynamic model of interconnected Lotka–Volterra systems has been developed both with static and delayed interconnections. It has been shown that the overall model of the networked LV system is a quadratic, i.e. a higher-order LV system. We have shown that the X-transformed model of interconnected Lotka–Volterra systems naturally admits a quasi-polynomial representation, facilitating systematic analysis and control design.

In order to analyze local asymptotic stability around a positive equilibrium, we have shown that the X-factorable transformation preserves local diagonal stability. This implies the local asymptotic stability of the positive equilibrium points of both the original and the transformed system model.

We propose a decentralized setpoint-tracking controller design based on the transformed model that guarantees population persistence in the subsystems of the network. The proposed controller design is computationally simple and ensures that the controlled system is locally diagonally stable around the prescribed setpoint. Moreover, larger controller gains improve disturbance attenuation, mitigating the effect of the disturbance term on control performance.

A simple simulation case study is used to demonstrate and validate the proposed theoretical modeling and control framework.

Use of AI tools declaration

The authors declare they have not used Artificial Intelligence (AI) tools in the creation of this article.

Acknowledgments

This study was supported by the National Research, Development, and Innovation Fund of Hungary, financed under the K_23 funding scheme, project no. 145934. The research work of L. Márton was also supported by the Domus Scholarship of Hungarian Academy of Sciences.

Conflict of interest

The authors declare there are no conflict of interest.

References

1. Y. Takeuchi, *Global Dynamical Properties of Lotka-Volterra Systems*, World Scientific Publishing, Singapore, 1996.
2. S. Chen, J. Shi, Z. Shuai, Y. Wu, Global dynamics of a Lotka–Volterra competition patch model, *Nonlinearity*, **35** (2021), 817. https://doi.org/10.1088/1361-6544/ac3c2e
3. M. AlAdwani, S. Saavedra, Is the addition of higher-order interactions in ecological models increasing the understanding of ecological dynamics?, *Math. Biosci.*, **315** (2019), 108222. https://doi.org/10.1016/j.mbs.2019.108222
4. E. Bairey, E. D. Kelsic, R. Kishony, High-order species interactions shape ecosystem diversity, *Nat. Commun.*, **7** (2016), 12285. https://doi.org/10.1038/ncomms12285

5. P. Singh, G. Baurah, Higher order interactions and species coexistence, *Theor. Ecol.*, **14** (2021), 71–83. https://doi.org/10.1007/s12080-020-00481-8
6. S. Cui, Q. Zhao, H. Jardon-Kojakhmetov, M. Cao, Species coexistence and extinction resulting from higher-order Lotka-Volterra two-faction competition, in: *Proc. IEEE Conf. Decis. Control*, 2023, 467–472. https://doi.org/10.1109/CDC49753.2023.10384227
7. T. Gibbs, S. A. Levin, J. M. Levine, Coexistence in diverse communities with higher-order interactions, *PNAS*, **119** (2022), e2205063119. https://doi.org/10.1073/pnas.2205063119
8. B. Hernández-Bermejo, V. Fairén, Lotka-Volterra representation of general nonlinear systems, *Math. Biosci.*, **140** (1997), 1–32. https://doi.org/10.1016/S0025-5564(96)00131-9
9. L. Brenig, A. Goriely, Universal canonical forms for time-continuous dynamical systems, *Phys. Rev. A*, **40** (1989), 4119. https://doi.org/10.1103/PhysRevA.40.4119
10. D. Frezzato, Universal embedding of autonomous dynamical systems into a Lotka-Volterra-like format, *Phys. Scr.*, **99** (2024), 015235. https://doi.org/10.1088/1402-4896/ad1236
11. Y. Takeuchi, Global stability in generalized Lotka-Volterra diffusion systems, *J. Math. Anal. Appl.*, **116** (1986), 209–221. https://doi.org/10.1016/0022-247X(86)90053-3
12. V. A. Jansen, A. L. Lloyd, Local stability analysis of spatially homogeneous solutions of multi-patch systems, *J. Math. Biol.*, **41** (2000), 232–252. https://doi.org/10.1007/s002850000048
13. L. Shen, R. Van, Predator–prey–subsidy population dynamics on stepping-stone domains, *J. Theor. Biol.*, **420** (2017), 241–258. https://doi.org/10.1016/j.jtbi.2017.03.013
14. G. Stépán, *Retarded dynamical systems: stability and characteristic functions*, Longman Scientific & Technical, 1989.
15. J. M. Cushing, *Integrodifferential equations and delay models in population dynamics*, vol. 20, Springer Science & Business Media, 2013.
16. T. Erneux, *Applied delay differential equations*, vol. 3, Springer Science & Business Media, 2009.
17. F. Chen, On a nonlinear nonautonomous predator–prey model with diffusion and distributed delay, *J. Comput. Appl. Math.*, **180** (2005), 33–49. https://doi.org/10.1016/j.cam.2004.10.001
18. J. A. Jacquez, C. P. Simon, Qualitative theory of compartmental systems with lags, *Math. Biosci.*, **180** (2002), 329–362. https://doi.org/10.1016/S0025-5564(02)00131-1
19. C. Chen, X.-W. Wang, Y.-Y. Liu, Stability of ecological systems: A theoretical review, *Phys. Rep.*, **1088** (2024), 1–41. https://doi.org/10.1016/j.physrep.2024.08.001
20. B. Hernández-Bermejo, Stability conditions and Liapunov functions for quasi-polynomial systems, *Appl. Math. Lett.*, **15** (2002), 25–28. https://doi.org/10.1016/S0893-9659(01)00087-8
21. N. Motee, B. Bamieh, M. Khammash, Stability analysis of quasi-polynomial dynamical systems with applications to biological network models, *Automatica*, **48** (2012), 2945–2950. https://doi.org/10.1016/j.automatica.2012.06.094
22. A. Figueiredo, I. Gleria, T. Rocha Filho, Boundedness of solutions and Lyapunov functions in quasi-polynomial systems, *Phys. Lett. A*, **268** (2000), 335–341. https://doi.org/10.1016/S0375-9601(00)00175-4

23. A. Magyar, G. Szederkényi, K. M. Hangos, Globally stabilizing feedback control of process systems in generalized Lotka–Volterra form, *J. Process Control*, **18** (2008), 80–91. https://doi.org/10.1016/j.jprocont.2007.05.003

24. A. Fradkov, I. Pchelkina, M. Ananyevskiy, A. Tomchin, Control of oscillations by control of invariants in quasi-polynomial nonlinear systems, *Nonlinear Dyn.*, **111** (2023), 13955–13967. https://doi.org/10.1007/s11071-023-08566-9

25. L. Márton, K. M. Hangos, A. Magyar, Passivity of Lotka–Volterra and quasi-polynomial systems, *Nonlinearity*, **34** (2021), 1880–1899. https://doi.org/10.1088/1361-6544/abd52b

26. A. Slavik, Lotka-Volterra competition model on graphs, *SIAM J. Appl. Dyn. Syst.*, **19** (2020), 725–762. https://doi.org/10.1137/19M1276285

27. J. Liu, X. Chen, D. Muñoz de la Peña, P. D. Christofides, Sequential and iterative architectures for distributed model predictive control of nonlinear process systems, *AlChE J.*, **56** (2010), 2137–2149. https://doi.org/10.1002/aic.12155

28. P. D. Christofides, R. Scattolini, D. Muñoz de la Peña, J. Liu, Distributed model predictive control: A tutorial review and future research directions, *Comput. Chem. Eng.*, **51** (2013), 21–41. https://doi.org/10.1016/j.compchemeng.2012.05.011

29. S. Chen, Z. Wu, P. D. Christofides, Decentralized machine-learning-based predictive control of nonlinear processes, *Chem. Eng. Res. Des.*, **162** (2020), 45–60. https://doi.org/10.1016/j.cherd.2020.07.019

30. L. Dong, Y. Takeuchi, Impulsive control of multiple Lotka-Volterra systems, *Nonlinear Anal. Real World Appl.*, **14** (2013), 1144–1154. https://doi.org/10.1016/j.nonrwa.2012.09.006

31. A. S. Anish, B. D. Baets, S. Rao, Metapopulation models with anti-symmetric Lotka-Volterra systems, *J. Biol. Dyn.*, **18** (2024), 2397404. https://doi.org/10.1080/17513758.2024.2397404

32. A. Muhammadhaji, A. Halik, H.-L. Li, Dynamics in a ratio-dependent Lotka-Volterra competitive-competitive-cooperative system with feedback controls and delays, *Adv. Differ. Equations*, **2021** (2021), 230. https://doi.org/10.1186/s13662-021-03364-2

33. Y. Muroya, Global stability of a delayed nonlinear Lotka-Volterra system with feedback controls and patch structure, *Appl. Math. Comput.*, **239** (2014), 60–73. https://doi.org/10.1016/j.amc.2014.04.036

34. T. Khan, H. Chaudhary, Estimation and identifiability of parameters for generalized Lotka-Volterra biological systems using adaptive controlled combination difference anti-synchronization, *Differ. Equations Dyn. Syst.*, **28** (2020), 515–528. https://doi.org/10.1007/s12591-020-00534-8

35. L. Márton, K. M. Hangos, A. Magyar, Migration-connected networks of Lotka-Volterra and quasi-polynomial systems, *Nonlinear Dyn.*, **113** (2025), 10577–10596. https://doi.org/10.1007/s11071-024-10619-6

36. N. Samardzija, L. D. Greller, E. Wasserman, Nonlinear chemical kinetic schemes derived from mechanical and electrical dynamical systems, *J. Chem. Phys.*, **90** (1989), 2296–2304. https://doi.org/10.1063/1.455970

37. K. P. Hadeler, *Topics in Mathematical Biology*, Springer, 2017.

38. G. Szederkényi, A. Magyar, K. M. Hangos, *Analysis and Control of Polynomial Dynamic Models with Biological Applications*, Academic Press, Cambridge, Massachusetts, 2018.

39. T. Plesa, Mapping dynamical systems into chemical reactions, *Nonlinear Dyn.*, **113** (2025), 31149–31173. https://doi.org/10.1007/s11071-025-11622-1

40. G. Cross, Three types of matrix stability, *Linear Algebra Appl.*, **20** (1978), 253–263. https://doi.org/10.1016/0024-3795(78)90021-6

41. L. Márton, G. Szederkényi, K. M. Hangos, Modeling and control of networked kinetic systems with delayed interconnections, *J. Process Control*, **130** (2023), 103084. https://doi.org/10.1016/j.jprocont.2023.103084

AIMS Press